



Dauner, A. L. L., Naafs, B. D. A., Pancost, R., & Martins, C. C. (2021). Exploring the application of TEX86 and the sources of organic matter in the Antarctic coastal region. *Organic Geochemistry*, 160, [104288]. <https://doi.org/10.1016/j.orggeochem.2021.104288>

Peer reviewed version

License (if available):
CC BY-NC-ND

Link to published version (if available):
[10.1016/j.orggeochem.2021.104288](https://doi.org/10.1016/j.orggeochem.2021.104288)

[Link to publication record in Explore Bristol Research](#)
PDF-document

This is the author accepted manuscript (AAM). The final published version (version of record) is available online via

Elsevier at <https://doi.org/10.1016/j.orggeochem.2021.104288> . Please refer to any applicable terms of use of the publisher.

University of Bristol - Explore Bristol Research

General rights

This document is made available in accordance with publisher policies. Please cite only the published version using the reference above. Full terms of use are available:
<http://www.bristol.ac.uk/red/research-policy/pure/user-guides/ebr-terms/>

Manuscript:

Exploring the application of TEX₈₆ and the sources of organic matter in the Antarctic coastal region

Ana Lúcia L. Dauner ^{a,b,1,*}, B. David A. Naafs ^c, Richard D. Pancost ^{c,d,e}, César C. Martins ^{a,*}

^a Center for Marine Studies, Federal University of Paraná, 83255-976 Pontal do Paraná, PR, Brazil

^b Graduate Program in Coastal and Oceanic Systems (PGSISCO) of the Federal University of Paraná, 83255-976 Pontal do Paraná, PR, Brazil

^c Organic Geochemistry Unit, School of Chemistry, University of Bristol, Bristol BS8 1TS, UK

^d Cabot Institute for the Environment, University of Bristol, Bristol BS8 1UJ, UK

^e School of Earth Sciences, University of Bristol, Bristol BS8 1RL, UK

¹ Current institution: Environmental Change Research Unit (ECRU), Ecosystems and Environment Research Programme, Faculty of Biological and Environmental Sciences, 00014, University of Helsinki, Helsinki, Finland.

* Corresponding author: anadauner@gmail.com (A.L.L. Dauner)
ccmart@ufpr.br (C.C. Martins)

25 **Highlights**

- 26 > Five GDGT-based calibrations were tested against reanalysis temperatures.
- 27 > The best fit was obtained using with a quadratic calibration.
- 28 > The GDGT-based sea surface temperature (SST) represented the Oct/Nov/Dec season.
- 29 > Organic matter input was controlled mainly by SST, precipitation and glacier retreat.

30

Abstract

Isoprenoidal glycerol dialkyl glycerol tetraethers (isoGDGTs) are archaeal biomarkers. In many settings, the degree of cyclization of isoGDGTs is correlated with temperature, forming the basis of the TEX₈₆ paleothermometer that is widely used to reconstruct sea surface temperature (SST) across a range of time scales. However, the application of TEX₈₆ to the polar regions is relatively limited and there is currently no consensus on which calibration is best suited for polar environments. In addition, application of TEX₈₆ to the polar regions is complicated by uncertainty regarding the source of organic matter input in coastal polar environments. We tested five different calibrations for TEX₈₆ in marine sediments from the Antarctic coastal region of Admiralty Bay near King George Island, using four short cores that span the second half of the 20th century. We also explored the possible sources of organic matter in these cores using sterol biomarkers. Best results for TEX₈₆ were obtained using a quadratic calibration. The TEX₈₆ signal presented a strong seasonal signal and best matched reanalysis temperatures of the austral spring season (Oct/Nov/Dec). The most abundant compounds observed in the sediments were the sterols cholest-5-en-3 β -ol and 24-ethylcholest-5-en-3 β -ol, the fatty alcohols C₁₆ and phytol, and isoGDGT-0, indicating a dominant marine origin of the organic matter. Differences in their vertical distributions suggests that some compounds (such as cholest-5-en-3 β -ol and phytol) may have had different sources over the evaluated period. Together our results indicate that TEX₈₆ can be used to reconstruct SSTs in the Antarctic coastal region.

Keywords: GDGT, sterol, sea surface temperature; organic matter; Admiralty Bay.

1. Introduction

Several biomarkers-based proxies have been developed for the reconstruction of sea surface temperature and organic matter (OM) production in the marine environment (Volkman, 2006; Eglinton and Eglinton, 2008; Schouten et al., 2013). A main focus has been on the isoprenoidal glycerol dialkyl glycerol tetraethers (isoGDGTs) produced by Archaea. The degree of cyclization of isoGDGTs is correlated with temperature in both laboratory cultures (De Rosa et al., 1980) and natural samples (Schouten et al., 2002; Kaur et al., 2015). This forms the basis for the TEX₈₆ paleothermometer (Schouten et al., 2002, 2013) that is widely used to reconstruct sea surface temperature (SST) across a range of time scales and as far back as the early Jurassic (e.g. Hertzberg et al., 2016; Robinson et al., 2017; Petrick et al., 2018). However, other factors can also influence the degree of cyclization of isoGDGTs under specific conditions (Pearson et al., 2004; Elling et al., 2015).

TEX₈₆ can be particularly useful in locations where other proxies cannot be easily applied, such as in the Southern Ocean and Antarctic shelf (Ho et al., 2014). However, the application of TEX₈₆ to the polar regions is still relatively limited and there is currently no consensus on which calibration is best suited for polar environments (Etourneau et al., 2013; Tierney and Tingley, 2014; Park et al., 2019). There are only a few studies that test the application of TEX₈₆ calibrations in the Antarctic and Southern Ocean environments and most of them used sediments recovered from the open ocean (e.g. Ho et al., 2014 and Fietz et al., 2016). An exception is the study by Jaeschke et al. (2017) that analyzed surface sediment samples encompassing a large range of latitudes (between 36° S and 68° S), including the Southern Ocean. Nevertheless, only a few of them were located below the Antarctic Polar Front, and all samples from the polar region (> 60° S) overestimated SST by up to 6 °C. The authors suggested the influence of seasonality and terrestrial input as explanations for this large bias in their polar samples.

Some studies adapted pre-existing calibrations to develop regional models for the Antarctic polar environment. Shevenell et al. (2011) modified the calibration model of Schouten et al. (2002) and suggested a regional calibration for the Antarctic Peninsula. More recently, Park et al. (2019) studied the seasonal effect on the GDGT-based thermometry from the Antarctic Polar Front. Based on the global calibration proposed by Kim et al. (2010), they concluded that there is a nonlinear relationship between TEX₈₆^L and SST, and proposed a quadratic calibration for Antarctic environments south of 50° S.

87 However, a thorough assessment of the performance of these calibrations to the Antarctic
88 environment is so far lacking.

89 In addition to the choice of the calibration method, the TEX₈₆^L –based SST
90 reconstructions can also be affected by environmental conditions other than temperature,
91 as mentioned earlier. Some studies identified that high productive regions and/or periods
92 may affect the SST reconstruction (Hurley et al., 2018; Park et al., 2018). Although
93 several studies have used biomarkers to reconstruct marine productivity and identify the
94 sources of OM in Antarctic marine sediments (Huang et al., 2011; Wisniewski et al., 2014;
95 Ceschim et al., 2016), none of the calibration studies in the Antarctic region evaluated the
96 effect of variations in the OM productivity in the TEX₈₆^L –based SST paleothermometry.

97 In this context, understanding the environmental forcing and marine
98 biogeochemical processes in polar environments involving the distribution and
99 composition of sedimentary OM in general - and isoGDGT distributions specifically - is
100 of high priority, and potentially able to assist in the understanding of local environmental
101 changes (Shetye et al., 2017; Henley et al., 2019). The main objective of this work is to
102 evaluate the OM character and sources, isoGDGT distributions and the performance of
103 the TEX₈₆ proxy in several short sediment cores from Admiralty Bay, located in the Sub-
104 Antarctic sector, that span the second half of the 20th century. To evaluate the performance
105 of the TEX₈₆ proxy, several existing calibrations of the GDGT-based paleothermometer
106 were tested to reconstruct sea surface temperature and compared to the available
107 reanalysis record.

109 2. Study Area

110 Admiralty Bay is a glacial fjord, centrally located within King George Island
111 (KGI), in the western region of the Antarctic Peninsula (Fig. 1). The island is mostly
112 formed of volcanic rocks of Late Cretaceous to Early Tertiary (Paleocene - Oligocene)
113 ages, which are related to the subduction of the SE-Pacific oceanic crust underneath the
114 Antarctic Continent (Smellie et al., 1984; Machado et al., 2001). Mafic volcanic rocks
115 (i.e. basalts, basalt-andesites and andesites) are the dominant lithologies. Rhyolite and
116 dacite are less abundant (Machado et al., 1998).

117 In 1999, the KGI was more than 90% covered by ice fields, and the ice-free areas
118 were concentrated along the coast (Simões et al., 1999). Due to regional warming, several
119 glaciers have now retreated out of the sea. Between 2000 and 2008, the loss amounted to
120 about 20 km², about 1.6% of the total area of the island (Rückamp et al., 2011). The

Admiralty Bay has an area of ca. 120 km², and it is composed of three branches: Ezcurra Inlet (E.I.) to the south-west, Mackellar Inlet (Mk.I.) to the north, and Martel Inlet (Mt.I.) to the north-east (Rakusa-Suszczewski, 1995). The water depth varies from shallow water up to 530 m deep, with an average depth of ca. 200 m (Rakusa-Suszczewski, 1995).

Surface sediments are heterogeneous, displaying coarse sediments (gravel and sand) mainly at the external and central parts of the bay (Fávaro et al., 2011). Ezcurra and Mackellar inlets display great heterogeneous grain size spatial distribution with sand content ranging between 6 and 60%. Sediments from Martel Inlet are predominantly composed of silt and clay fractions with percentages higher than 70% (Martins et al., 2005; Berbel and Braga, 2014).

The observed mean annual air temperature on the KGI was - 2.5 C° between 1948 and 2011 (Kejna et al., 2013). During austral Summer and also regularly during the Spring and Autumn months, air temperatures rise to well above freezing (Rückamp et al., 2011). Winds constitute a main meteorological feature and they influence the ablation rates, the surface energy fluxes (and therefore, the air temperatures), the water circulation and the resuspension of previously deposited material in the area (Braun et al., 2001, 2004; Pichlmaier et al., 2004). The precipitation on KGI is characterized by substantial interannual variability (Kejna et al., 2013) and affects the water column stratification and the resuspension of previously deposited material (Pichlmaier et al., 2004).

Hydrological conditions in Admiralty Bay are mainly driven by the exchange of water with the Bransfield Strait, freshwater runoff, and local processes in the fjord. The water flow can be described as tidal currents and superimposed wind driven currents (Robakiewicz and Rakusa-Suszczewski, 1999). The influence of wind and tidal variations on circulation is more intense in shallow areas, especially at the western side of the bay (Robakiewicz and Rakusa-Suszczewski, 1999) where wind plays an important role in upwelling that drives primary production (Brandini and Rebello, 1994). Freshwater runoff influences water column turbidity through the suspension of soft sediments in the region (Pichlmaier et al., 2004), and this runoff, enriched with guano and fragments of macroalgae, can be an important source of OM and nutrients to the bay (Nędzarek, 2008).

3. Material and Methods

3.1. Sampling

Four short sediment cores (BTP - Botany Point; REF - Refuge II; STH - Stenhouse; THP - Thomas Point) (red dots, Fig. 1 and Table 1) were collected during the

XXV Brazilian Antarctic Expedition (summer 2006/2007) using a mini-box corer (25 * 25 * 55 cm) (Ferreira et al., 2013; Martins et al. , 2010, 2014). The cores were generally sectioned every 1 cm, and the samples were first stored at - 20 °C in previously calcined aluminum trays. Samples for the analysis of radionuclides were stored in plastic containers. Samples for the analysis of organic markers were freeze-dried, homogenized in a mortar and stored in glass vials until laboratory analysis.

3.2. Age Model

The activity of radionuclide ^{137}Cs was determined by gamma spectrometry with hyper-pure Germanium detector (model GEM60190, EGG & ORTEC) and the vertical variation was used to estimate sedimentation rates. The detailed methods were first published by Martins et al. (2010) and Ferreira et al. (2013) and the obtained sedimentation rates are presented in Table 1.

3.3. Total Organic Carbon (TOC)

TOC analysis was conducted using 1.0 g of homogenized sediments. Samples were pre-treated with hydrochloric acid, washed twice with deionized water to remove chloride, and dried at 80 °C overnight. The TOC was determined using a Carlo Erba 1100 CHN Analyser with a precision of ± 0.1 wt %. Measurements were performed in duplicate and the average is reported here.

3.4. Sample extraction, instrumental analysis and analytical control

The analytical method used to extract the biomarkers (GDGTs, fatty alcohols and sterols) consisted of ultrasonic extraction and alumina column fractionation. For this purpose, dried sediments (ca. 10 - 15 g) were ultrasonically extracted with dichloromethane (DCM; 2 times), DCM: methanol (MeOH) (1:1; v/v; 2 times) and MeOH (2 times). The extracts were combined and evaporated to dryness and then fractionated using solid phase extraction method and short alumina columns. The apolar fraction was eluted with approximately 4.5 mL *n*-hexane: DCM (9:1, v/v), while the polar fraction (containing the compounds of interest here) was eluted with approximately 6 mL DCM:MeOH (1:2; v/v). The polar fraction was further divided into two portions, one for the analysis of branched and isoprenoidal GDGTs and one for the analysis of fatty alcohols and sterols. These extracts were dried under N_2 flow. The fraction for GDGT analysis was resuspended in *n*-hexane: isopropanol (99: 1, v/v); filtered (PTFE filter, 0.45

189 μm); and concentrated to about 2 mg mL^{-1} prior to LC-MS analysis. The other portion
190 destined for the analysis of fatty alcohols and sterols by GC-MS was derivatized using
191 BSTFA and pyridine (heating at 70°C for 1 h).

192 GDGTs were analyzed by high performance liquid chromatography coupled with
193 atmospheric pressure chemical ionization mass spectrometry (HPLC-APCI-MS, Thermo
194 Finnigan TSQ/Acela Series). All samples were measured in triplicate and the average
195 values are reported here. Chromatographic separation of compounds was achieved using
196 an Alltech Prevail Cyano column ($2.1 \text{ mm i.d.} \times 150 \text{ mm}$, $3 \mu\text{m}$). The GDGTs were eluted
197 isocratically with *n*-hexane: isopropanol (99: 1, v/v) for 7 min, followed by a linear
198 gradient to 1.3% isopropanol at 30 min, to 1.6% isopropanol at 35 min, then increasing
199 to 10% isopropanol at 36 min and kept for 8 min (at a flow of 0.2 mL min^{-1}), finally
200 equilibrating with 1% isopropanol for 13 min before the next injection. After each three
201 analyses, the column was cleaned by back-flushing of *n*-hexane: isopropanol (99: 1, v/v)
202 for 7 min and then rinsed by a linear gradient from 9: 1 (v/v) to 99: 1 (v/v) *n*-hexane:
203 isopropanol within 14 min and equilibrated with 1% isopropanol at 30 min. The
204 instrumental conditions for APCI-MS were: drying gas (N_2) flow 6 L min^{-1} and
205 temperature 200°C , vaporizer temperature of 380°C , capillary temperature of 282°C
206 and corona discharge current of $3 \mu\text{A}$. GDGTs were detected by APCI/MS in selected ion
207 monitoring (SIM) mode (m/z 1302, 1300, 1298, 1296, 1292, 1050, 1048, 1046, 1036,
208 1034, 1032, 1022, 1020, 1018, 653 and 744). GDGTs were semi-quantified with an
209 interval synthetic C_{46} tetraether standard.

210 The fatty alcohols and the sterols were analyzed by gas chromatography-mass
211 spectrometry (GC-MS; ThermoQuest Trace GC interfaced to Finnigan Trace MS
212 quadrupole spectrometer). Separation was achieved using a HP-1 fused silica capillary
213 column ($50 \text{ m} \times 0.32 \text{ mm i.d.}$; $0.17 \mu\text{m}$ film thickness). The injection was made at 70°C
214 and the temperature increased to 130°C at $20^\circ\text{C min}^{-1}$, then up to 300°C at 4°C min^{-1} ,
215 and then remained constant at 300°C for 20 min. Helium was used as a carrier gas. The
216 GC-MS operated in electron impact ionization (70 eV) and full scan mode (m/z 50-650).
217 The internal standard to quantify the fatty alcohols and sterols was 2-hexadecane, added
218 prior to GC-MS analysis. The analyte peak areas were integrated from the total ion current
219 chromatograms.

3.5. Data analysis

The statistical analyses were performed in R version 3.5.1 (R Core Team, 2018) using the packages Hmisc (Harrell Jr., 2019), pracma (Borchers, 2019) and WaveletComp (Roesch and Schmidbauer, 2018), while the spatial analyses were performed using the QGIS 3.4.2 software (QGIS Development Team, 2018).

First, we calculated four different indices to test if there are any potential sources other than the planktonic Thaumarchaeota that could affect the GDGT-based paleothermometry interpretation. The Branched and Isoprenoid Tetraether Index (BIT) was proposed by Hopmans et al. (2004) to evaluate the relative input of terrestrial OM in the marine environment.

$$\text{BIT} = ([\text{brGDGT-I}] + [\text{brGDGT-II}] + [\text{brGDGT-III}]) / ([\text{crenarchaeol}] + [\text{brGDGT-I}] + [\text{brGDGT-II}] + [\text{brGDGT-III}])$$

The methane index (MI) was proposed by Zhang et al. (2011) to indicate the relative contribution of GDGTs derived from methanotrophic Archaea to those from planktonic Thaumarchaeota.

$$\text{MI} = ([\text{isoGDGT-1}] + [\text{isoGDGT-2}] + [\text{isoGDGT-3}]) / ([\text{isoGDGT-1}] + [\text{isoGDGT-2}] + [\text{isoGDGT-3}] + [\text{crenarchaeol}] + [\text{cren. isomer}])$$

The ring index (RI) was proposed by Zhang et al. (2016) to indicate a potential non-thermal influence on GDGTs distributions. $|\Delta\text{RI}|$ indicates the residual of a sample's RI ($\text{RI}_{\text{sample}}$) from a calculated RI ($\text{RI}_{\text{calculated}}$) based on the global TEX_{86} – RI regression.

$$\text{RI}_{\text{sample}} = 0 * \{\text{isoGDGT-0}\} + 1 * \{\text{isoGDGT-1}\} + 2 * \{\text{isoGDGT-2}\} + 3 * \{\text{isoGDGT-3}\} + 4 * \{\text{crenarchaeol}\} + 4 * \{\text{cren. isomer}\}$$

$$\text{RI}_{\text{calculated}} = -0.77 (\pm 0.38) * \text{TEX}_{86} + 3.32 (\pm 0.34) * (\text{TEX}_{86})^2 + 1.59 (\pm 0.10)$$

$$|\Delta\text{RI}| = \text{RI}_{\text{calculated}} - \text{RI}_{\text{sample}}$$

Lastly, the % GDGT-0 was proposed by Sinninghe Damsté et al. (2012) to indicate the contribution of methanogenic Archaea.

$$\%GDGT-0 = [\text{isoGDGT-0}] / ([\text{isoGDGT-0}] + [\text{crenarchaeol}])$$

While the MI and %-GDGT-0 indices were calculated based on the compounds' abundance (brackets), the RI index was calculated based on the percentage of the compounds (braces).

The TEX₈₆ index was calculated following Schouten et al. (2002):

$$\text{TEX}_{86} = ([\text{isoGDGT-2}] + [\text{isoGDGT-3}] + [\text{cren. isomer}]) / ([\text{isoGDGT-1}] + [\text{isoGDGT-2}] + [\text{isoGDGT-3}] + [\text{cren. isomer}])$$

In addition, we also calculated the TEX₈₆^L index (Kim et al., 2010):

$$\text{TEX}_{86}^L = \log_{10} ([\text{isoGDGT-2}] / ([\text{isoGDGT-1}] + [\text{isoGDGT-2}] + [\text{isoGDGT-3}]))$$

To verify the applicability of the GDGT-based paleotemperature proxies to the polar environment, calculated temperatures based on the sediment cores GDGT data were compared with the interpolated mean temperature taken from the Simple Ocean Data Assimilation (SODA3) reanalysis data (Carton and Giese, 2008) (<http://dsrs.atmos.umd.edu/DATA/soda3.3.2>). The data are initially based on a numerical model and then corrected based on direct observations. They have a final horizontal resolution of 0.25° * 0.25° and cover the period between 1980 and 2015 (Carton et al., 2018). The GDGT-based temperatures were compared with the annual mean and seasonal temperatures (from 1980 to 2006) corresponding to the nearest interpolated 0.50° gridbox (average of the surrounding four grid cells). To explore the influence of seasonality, we calculate quarterly averages, using different combinations of months. For example, the “summer 1” season was formed by the December, January and February months (the usual combination); the “summer 2” combination was formed by January, February and March; and the “summer 3” combination was formed by February, March and April. Finally, the fit between GDGT-based SST and satellite-based SST was tested using the Spearman correlation test because not all datasets were normally distributed. The five GDGT-based SST calibrations we tested here were proposed by Kim et al. (2010), Shevenell et al. (2011), Tierney and Tingley (2014), Park et al. (2019), and Dunkley Jones et al. (2020).

All plots from the Bellingshausen Station (see Fig. 1) are based on data from the Antarctic Research and Investigation subprogram, obtained from the READER (Reference Antarctic Data for Environmental Research), a project of the Scientific Committee on Antarctic Research (AARI, 2019). The precipitation data are presented as monthly sums (in mm), while the wind speeds are presented as monthly means (in m^{-1}).

4. Results

4.1. OM input

The BTP is the longest sediment core with the highest temporal resolution. Therefore, we analyzed the OM variation and its dependence on SST and other environmental parameters using this record only. In this core that spans the last 50 years, there is a similar trend in concentration for the sterols, alcohols, and isoGDGTs and this trend is also similar to that seen in the TOC record (Fig. 2). At first (~ 1963 to 1975), the concentrations decreased, followed by a gradual increase between 1975 and 1998. The input slightly decreased after 2000.

The dominant sterols were cholest-5-en-3 β -ol (cholesterol; $27\Delta^5$) and 24-ethylcholest-5-en-3 β -ol (sitosterol; $29\Delta^5$). (Fig. 3). The 5 α -stanols were less abundant than their unsaturated analogues, being normally diagenetically produced by the microbial reduction of Δ^5 -stenols into 5 α -stanols (Grimalt et al., 1990). The ratio 5 α -stanols/ Δ^5 -stenols was generally higher than 0.5. Other abundant compounds were the *n*-alkanol *n*-C₁₆-OH and phytol. All sediments contained isoGDGTs. The main GDGTs found in our sampling site were GDGT-0 and crenarchaeol, representing around 50% and 40% of the isoGDGT distribution, respectively.

4.2. IsoGDGTs and calibration of the SST estimates

Various indices have been proposed to characterize the source of sedimentary isoGDGTs (and, by extension, their suitability for SST reconstruction). GDGTs can be derived from terrestrial sources or be produced in the water column and/or within sediments (Sinninghe Damsté et al., 2012; Schouten et al., 2013; Zhang et al., 2016). The Branched and Isoprenoid Tetraether Index (BIT) indicates the terrestrial input of GDGTs to marine sediments when it exceeds 0.3 (Hopmans et al., 2004; Weijers et al., 2006). Overall, the BIT varied between 0.04 and 0.07 at BTP sediment core (Supplementary

Table S1), suggesting that effect of the fluvial input of terrestrially derived isoprenoid GDGTs on the GDGT-based paleothermometry may be negligible.

The methane index (MI) indicates the relative contribution of GDGTs derived from methanotrophic Archaea (Zhang et al., 2011), when its values exceed 0.3. The MI in our samples was low with a maximum of 0.07 (Supplementary Table S1). Similarly, the % GDGT-0 indicates the contribution of methanogenic Archaea when it exceeds 67% (Sinninghe Damsté et al., 2012). These varied between 44 and 88% across the four cores. For the BTP, REF and THP cores all sediments had values < 67%. The STH core had 6 samples between 4.5 and 12.5 cm deep (spanning the years 1977-1994), with a % GDGT-0 > 67% (Supplementary Table S1).

The ring index residual ($|\Delta RI|$) is less clearly linked to specific biological sources but it indicates a non-temperature influence on GDGT distributions when it exceeds 0.3 (Zhang et al., 2016). The $|\Delta RI|$ varied between 0.03 and 1.53. In the BTP, TEF and THP cores most samples had a $|\Delta RI|$ value < 0.3. Sediments from the STH core, those between 4.5 and 12.5 cm deep (spanning the years 1977-1994), all had values > 0.3 with maxima > 1 (Supplementary Table S1). Therefore, the BIT, MI, $|\Delta RI|$, and % isoGDGT-0 all indicate that the majority of isoGDGTs are produced within the water column. For the STH core, the indices suggest a contribution of archaeal groups other than the planktonic Thaumarchaeota to the isoGDGT pool.

We then determined the temperature estimates using five GDGT-based calibrations. These are the TEX₈₆^L calibration proposed by Kim et al. (2010) for (sub)polar oceans, the TEX₈₆ calibration developed by Shevenell et al. (2011) for the Antarctic Peninsula, the global BAYSPAR TEX₈₆ calibration (using the surface mode) of Tierney and Tingley (2014) that is based on a spatially-varying calibration model, the TEX₈₆^L calibration by Park et al. (2019) using a polynomial calibration for the Southern Ocean, and the OPTiMAL calibration proposed by Dunkley Jones et al. (2020) based on the distribution of six isoprenoid GDGTs. These temperatures can be compared to those obtained from the SODA reanalysis, considering the annual and seasonal means. Samples with MI, $|\Delta RI|$, and % isoGDGT-0 values above the thresholds were excluded from this analysis. The only quarterly combination that presented significant correlation values (p -value < 0.05) was: JFM = austral summer, AMJ = austral autumn, JAS = austral winter, OND = austral spring (Supplementary Table S2). The Spearman correlation analysis indicated that the best fit was achieved with the austral spring season (Oct-Nov-Dec) (Table 2).

Based on these results, we compared the SODA-based SST from the austral spring season (OND) with the temperature estimates obtained with the five calibration methods (Fig. 4). Using this approach, the AntPen calibration proposed by Shevenell et al. (2011) significantly overestimated the SST at all three locations. The OPTiMAL calibration by Dunkley Jones et al. (2020) also overestimated the SST at all three locations, whereas the TEX₈₆^L and BAYSPAR calibrations proposed by Kim et al. (2010) and Tierney and Tingley (2014), respectively, overestimated the SST only when the TEX₈₆ values exceeded 0.45. The quadratic calibration proposed by Park et al. (2019) provides the best fit with the reanalysis record.

5. Discussion

5.1. OM input and temporal evolution

As observed in Fig. 2, the OM proxies did not exhibit homogenous behaviors during the last 50 years. The differences among the biomarker records may have been caused by changes in the productivity of the source organisms. Thus, we first explored the source of the OM proxies before discussing their temporal evolution.

The most abundant sterol is the cholest-5-en-3 β -ol. It can be produced by phytoplankton and zooplankton, and is present in the feces of penguins and pinnipeds (Wisnieski et al., 2014). The similarity between the profiles of cholest-5-en-3 β -ol and 24-methylcholest-5,22E-dien-3 β -ol (brassicasterol; 28 $\Delta^{5,22}$; a marker for diatoms – Volkman, 1986) corroborates phyto- and zooplankton as the main sources for cholest-5-en-3 β -ol (Fig. 3). The only exception is the sample around the year 2004, when the peak of cholest-5-en-3 β -ol does not coincide with an increase in the methylcholest-5,22E-dien-3 β -ol input. During this period, cholest-5-en-3 β -ol probably had a significant contribution from penguin feces, since the regions of Ulmann Point and Keller Peninsula are used for penguins to molt their feathers (Weber and Montone, 2006). The second most abundant sterol is the 24-ethylcholest-5-en-3 β -ol (sitosterol; 29 Δ^5) (Fig. 3). This sterol predominance was also found by Wisnieski et al. (2014) in Admiralty Bay, and they attributed the 24-ethylcholest-5-en-3 β -ol to macro- and microalgae. The similarity between the profiles of 24-ethylcholest-5-en-3 β -ol and 24-methylcholest-5,22E-dien-3 β -ol corroborates the diatoms as the probable main source for the 24-ethylcholest-5-en-3 β -ol.

The main fatty alcohols are the *n*-alkanol *n*-C₁₆-OH and phytol (Fig. 3). The *n*-alkanol *n*-C₁₆-OH is usually associated with aquatic algae, bacteria and zooplankton (Wisnieski et al., 2014). However, the absence of similarity between the *n*-alkanol *n*-C₁₆-OH, cholest-5-en-3 β -ol, 24-methylcholest-5,22E-dien-3 β -ol and phytol suggests that this short-chain *n*-alkanol is neither derived from aquatic algae nor zooplankton, but probably from non-photosynthetic organisms, such as bacteria. Phytol (3,7,11,15-tetramethyl-2-hexadecen-1-ol), on the other hand, has been used as a marker of photosynthetic organisms since it is derived from the degradation of chlorophyll-*a* (Volkman et al., 2008). Its depth profile is similar to that of 24-methylcholest-5,22E-dien-3 β -ol, suggesting similar sources. However, high phytol concentrations between 1980 and 1985 are not accompanied by changes in the concentrations of other microalgae biomarkers (24-methylcholest-5,22E-dien-3 β -ol, 24-ethylcholest-5-en-3 β -ol and 4 α ,23,24-trimethylcholesta-22E-en-3 β -ol – dinosterol, 30 Δ ²²). This suggests an input from other photosynthetic producers, such as cyanobacteria or macroalgae.

Finally, as observed in Fig. 3, the ratio of 5 α -stanols/ Δ ⁵-stenols was generally higher than 0.5, suggesting significant alteration of the sedimentary OM due to bacterial activity (Wakeham and Canuel, 2006; Wisnieski et al., 2014). The values of the ratio 29 Δ ⁰/29 Δ ⁵ decreased from the bottom to the top of the sediment core, indicating a strong diagenetic activity after the final burial of OM in the sediment. The values of the ratio 27 Δ ⁰/27 Δ ⁵, on the other hand, presented higher values around 1970 and after 1990. Since the cholest-5-en-3 β -ol (27 Δ ⁵) and the 24-ethylcholest-5-en-3 β -ol (29 Δ ⁵) have distinct sources, the difference between the 5 α -stanols/ Δ ⁵-stenols profiles may indicate a preferential degradation between different organic compounds.

Regardless of source, most compounds (24-methylcholest-5,22E-dien-3 β -ol, 24-ethylcholest-5-en-3 β -ol, 4 α ,23,24-trimethylcholesta-22E-en-3 β -ol and phytol profiles in Fig. 4) indicate elevated phytoplankton productivity between 1963 and 1975, and between 2000 and 2006.

Between 2002 and 2009, Lange et al. (2015) also found significantly higher phytoplankton abundances in Botany Point compared to the region in front of Keller Peninsula. Among several parameters, they found that precipitation showed the largest influence over phytoplankton populations, with the most productive years coincident with high precipitation in summer. According to Nędzarek (2008), the main nutrient sources to the Admiralty Bay are the continental runoff of freshwater enriched in biogenic compounds from the penguin rookeries, and the decomposition of macroalgae. Thus, high

precipitation rates can increase the continental runoff, increasing nutrient supply to the coastal region. Lange et al. (2015) also observed a negative correlation between the wind speed and the phytoplankton abundance. Strong winds tend to increase the water turbidity, decreasing light penetration and primary production (Pichlmaier et al., 2004; Lange et al., 2015). The first precipitation and wind speed data for the King George Island were obtained at the Bellingshausen research station in 1968 (Fig. 5) (SCAR Reader Project, 2019). Based on the available data, the relatively low wind speed coupled to high precipitation in the late 1960s may have been responsible for the high marine productivity in the beginning of the record and its decreasing trend towards 1975 (Fig. 5).

Between 1976 and 1998, increase in algal biomarker abundances could have been caused by a slightly wetter and warming weather (Kejna et al., 2013). However, the large input of alcohols and isoprenoid GDGTs between 1980 and 1987 does not correspond to any of these parameters (precipitation in Fig. 5 and SST and Fig. 6). A possible explanation is glacier retraction. Between 1979 and 1988, Rosa et al. (2014) reported high area loss of the main glaciers around the BTP sampling site, especially the Krak glacier (Fig. 5, rightmost panel). The melted water may have carried continental nutrients to the coastal region.

After that, there was a relative stabilization in the OM input. The largest variation occurred in 2004, where the increase in sterol concentration was driven mainly by a peak in the cholest-5-en-3 β -ol concentrations. As discussed above, since this increase was not accompanied by a proportional increase in the phytoplankton biomarkers, it is more plausible that it is derived from penguin feces, instead of from the zooplankton. It suggests an increase in the population of ice-tolerant penguin species, such as gentoo penguins (Henley et al., 2019), around Botany Point. That may have been caused by the retreat of the glaciers, exposing ice-free land areas (Oliveira et al., 2019). This increase in the supply of ornithogenic nutrients, in turn, may have promoted the marine productivity.

5.2. IsoGDGTs and calibration of the SST estimates

As mentioned earlier, some caution should be taken before applying the GDGT-based indices to reconstruct temperature because of the possibility of alternative sources for the isoGDGTs other than planktonic Thaumarchaeota. When applied to the STH record, the RI indicated a potential non-thermal influence between 1977 and 1996, while

a potential contribution from methanogens was observed between 1984 and 1994 (Supplementary Table S1).

After discounting source effects, we found a strong positive correlation between GDGT-based SST and austral spring SST (Oct-Nov-Dec; Table 2). Only the calibration proposed by Dunkley Jones et al. (2020) did not exhibit a positive correlation with the annual or any of the seasonal means. In 2011, Nakayama et al. found that the archaeal communities in Martel Inlet are dominated by the phylum Thaumarchaeota (formerly known as Crenarchaeota), a major source of the isoprenoid GDGTs used in the TEX₈₆ calculation (Schouten et al., 2002, 2013). In 2015, Hernández et al. studied the marine archaeal community structure in Potter Cove, a shallow water coastal marine area located in the King George Island. They also observed a high dominance of members of the phylum Thaumarchaeota, specially during the spring. During this season, the increase in solar radiation and temperature promotes primary productivity. The warmer temperatures also increase freshwater run-off, delivering more suspended particulate matter (SPM) to the water column. The higher primary productivity rates coupled with the SPM input enhances the growth of Thaumarchaeota. More recently, Signori et al. (2018) studied the seasonal changes in bacterial and archaeal diversity and community structure in the Bransfield Strait. Their results indicate that seasonal variation of temperature and OM production are regulatory factors affecting the bacterial and archaeal communities. During spring, the phylum Thaumarchaeota represents an important fraction (more than 5%) of the microbial community. However, in the summer, its relative abundance drops to 1% or less, being outcompeted by bacteria. These microbial community dynamics likely explain the high correlation between the GDGT-based SSTs and the austral spring season SST.

Of five calibrations tested, that proposed by Park et al. (2019) presented the best fit to SODA-based SST from the austral spring season (OND) (Fig. 4). However, because it is a quadratic calibration, it could generate ambiguous values. The inflection of the calibration curve is around 7 °C and historical SST means do not exceed 2 °C (neither when analysing annual means nor spring means) (Supplementary Fig. S1). Thus, we assume that only the cold temperature estimates are accurate and used the calibration proposed by Park et al. (2019) in the subsequent analysis.

5.3. SST trends

Using the calibration proposed by Park et al. (2019), we calculated SST for the sediment core at BTP, since it is the longest one with the highest temporal resolution. The TEX₈₆-based temperatures from BTP, considering the calibration errors, are in the same range as the mean air temperatures observed in the King George Island by Kejna et al. (2013) (Fig. 6, top panel). The period between 1979 and 2000 had the largest observed glacier retreat in the Martel Inlet (Rosa et al., 2014). This warming trend is observed in the TEX₈₆-based SST records. After 1998, however, we detect no warming in the BTP record (Fig. 6, bottom panel), similar to observations of the Antarctic Peninsula by Turner et al. (2016) and Huai et al. (2019). Low SST values were observed around 1977, 1996 and 2004. They did not coincide with consistent patterns of decreased freshwater input, through either precipitation or meltwater inflow from the adjacent glaciers. However, these cooler periods coincided with relatively high wind speed values that may have promoted the water column mixture bringing colder waters to the surface (Fig. 5).

Finally, changes in the OM production did not affect the SST reconstruction. Hurley et al. (2018) found that the sedimentary TEX₈₆ values may under-predict local SST in regions of high productivity. After blooming episodes, common in polar environments, ammonia released by remineralization of organic matter may promote archaeal ammonia oxidation rate and growth rate. However, the correlations between SST values and the organic matter proxies in this study were low ($|R_s| < 0.17$) and non-significant (p -value < 0.05) (Supplementary Table S3). While the largest variations in the OM were observed mainly between 1965 and 1980, the largest SST variation occurred around the year 2000 (Fig. 5).

6. Conclusions

We evaluated the performance of the TEX₈₆ proxy in four short sedimentary cores collected in the Admiralty Bay, King George Island, that span the second half of the 20th century; we complemented that investigation with analyses of OM sources in the longest and most complete of these cores.

Combined with meteorological data, we were able to examine causes in dramatic and unexpected variations in primary productivity. Before 1975, the primary productivity was primarily driven by precipitation and wind dynamics. An increase in phytoplankton productivity occurred between 1985 and 2000, probably promoted by SST warming and

the relatively wetter climate. Glacier retreats near the sampling site may also have promoted the primary productivity, especially in the early 1980s and late 1990s. In the last part of the record, there was a relative stabilization in the OM input coupled with a cooling SST trend. The exception was around the year 2004, when a peak of cholesterol decoupled from environmental proxies and other biomarkers likely documents an increase in the contribution from “ice-tolerant” penguins.

As there are still no studies on the reconstruction of SST variations in the region, we tested five different calibrations developed for the Antarctic environment. The comparison between GDGT-based SST estimates (using five calibrations) and reanalysis-based SST (annual and seasonal means) indicated that the GDGT signal represents the austral spring season (Oct/Nov/Dec). The calibration that provided the best fit with the reanalysis-based SST was the quadratic calibration proposed by Park et al. (2019). Variations in OM production did not present any significant effect on the GDGT-based paleothermometry. This confirms the potential utility of GDGT-based SST proxies in this region and allowed us to develop a SST record from 1960 to 2010.

Acknowledgements

The work was supported by the Antarctic Brazilian Program (PROANTAR), Secretaria da Comissão Interministerial para os Recursos do Mar (SECIRM), Conselho Nacional de Desenvolvimento Científico e Tecnológico (CNPq, 550014/2007-1 and 442692/2018-8) and Coordenação de Aperfeiçoamento de Pessoal de Ensino Superior (CAPES, 88887.314458/2019-00). The authors wish to thank the ‘Comandante Ferraz’ Brazilian Antarctic Station staff for support during the sampling activities. B.D.A. Naafs acknowledges funding through a Royal Society Tata University Research Fellowship. NERC (Reference: CC010) and NEIF (www.isotopesuk.org) are thanked for funding and maintenance of the GC-MS and LC-MS instrument at the University of Bristol used for this work. C.C. Martins and A.L.L. Dauner thanks CAPES by personal grants support (BEX 5366/12-7 and 88887.362846/2019-00, respectively). Finally, this work is part of CARBMET project (The multiple faces of organic CARBOn and METals in the sub-Antarctic ecosystem) sponsored by CNPq, CAPES and Brazilian Ministry of Science, Technology, Innovation and Communication.

References

- AARI, 2019. Antarctic Research and Investigation (http://www.aari.aq/default_en.html) [WWW Document]. URL http://www.aari.aq/default_en.html (accessed 10.24.19).
- Berbel, G.B.B., Braga, E.S., 2014. Phosphorus in Antarctic surface marine sediments - Chemical speciation in Admiralty Bay. *Antarctic Science* 26, 281–289.
- Borchers, H.W., 2019. *pracma: Practical Numerical Math Functions*, v.2.2.5.
- Brandini, F.P., Rebello, J., 1994. Wind field effect on hydrography and chlorophyll dynamics in the coastal pelagial of Admiralty Bay, King George Island, Antarctica. *Antarctic Science* 6, 433–442.
- Braun, M.H., Saurer, H., Goßmann, H., 2004. Climate, energy fluxes and ablation rates on the ice cap of King George Island. *Pesquisa Antártica Brasileira* 103, 87–103.
- Braun, M.H., Saurer, H., Vogt, S., Simões, J.C., Goßmann, H., 2001. The influence of large-scale atmospheric circulation on the surface energy balance of the King George Island ice cap. *International Journal of Climatology* 21, 21–36.
- Carton, J.A., Chepurin, G.A., Chen, L., 2018. SODA3: A new ocean climate reanalysis. *Journal of Climate* 31, 6967–6983.
- Carton, J.A., Giese, B.S., 2008. A reanalysis of ocean climate using Simple Ocean Data Assimilation (SODA). *Monthly Weather Review* 136, 2999–3017.
- Ceschim, L.M.M., Dauner, A.L.L., Montone, R.C., Figueira, R.C.L., Martins, C.C., 2016. Depositional history of sedimentary sterols around Penguin Island, Antarctica. *Antarctic Science* 28, 443–454.
- De Rosa, M., Esposito, E., Gambacorta, A., Nicolaus, B., Bu'Lock, J.D., 1980. Effects of temperature on ether lipid composition of *Caldariella acidophila*. *Phytochemistry* 19, 827–831.
- Dunkley Jones, T., Eley, Y., Thomson, W., Greene, S.E., Mandel, I., Edgar, K.M., Bendle, J., 2020. OPTiMAL: a new machine learning approach for GDGT-based palaeothermometry. *Climate of the Past* 16, 2599–2617.
- Eglinton, T.I., Eglinton, G., 2008. Molecular proxies for paleoclimatology. *Earth and Planetary Science Letters* 275, 1–16.
- Elling, F.J., Könneke, M., Mußmann, M., Greve, A., Hinrichs, K.U., 2015. Influence of temperature, pH, and salinity on membrane lipid composition and TEX₈₆ of marine planktonic thaumarchaeal isolates. *Geochimica et Cosmochimica Acta* 171, 238–255.
- Etourneau, J., Collins, L.G., Willmott, V., Kim, J.H., Barbara, L., Leventer, A.,

- Schouten, S., Sinninghe Damsté, J.S., Bianchini, A., Klein, V., Crosta, X., Massé, G., 2013. Holocene climate variations in the western Antarctic Peninsula: Evidence for sea ice extent predominantly controlled by changes in insolation and ENSO variability. *Climate of the Past* 9, 1431–1446.
- Fávaro, D.I.T., Silva, P.S.C., Mazzilli, B.P., Cavallaro, G.P.M., Taddei, M.H.T., Berbel, G.B.B., Braga, E.S., 2011. Sediment geochemistry in Admiralty Bay (Antarctica): trace, rare earth elements and radionuclides. *Brazilian Antarctic Research* 5, 1–14.
- Ferreira, P.A.L., Ribeiro, A.P., Nascimento, M.G., Martins, C.C., Mahiques, M.M., Montone, R.C., Figueira, R.C.L., 2013. ¹³⁷Cs in marine sediments of Admiralty Bay, King George Island, Antarctica. *Science of the Total Environment* 443, 505–510.
- Fietz, S., Ho, S.L., Huguet, C., Rosell-Melé, A., Martínez-García, A., 2016. Appraising GDGT-based seawater temperature indices in the Southern Ocean. *Organic Geochemistry* 102, 93–105.
- Grimalt, J.O., Fernandez, P., Bayona, J.M., Albaigés, J., 1990. Assessment of fecal sterols and ketones as indicators of urban sewage inputs to coastal waters. *Environmental Science & Technology* 24, 357–363.
- Harrell Jr., F.E., 2019. Hmisc: Harrell Miscellaneous, v. 4.1.1.
- Henley, S.F., Schofield, O.M., Hendry, K.R., Schloss, I.R., Steinberg, D.K., Moffat, C., Peck, L.S., Costa, D.P., Bakker, D.C.E., Hughes, C., Rozema, P.D., Ducklow, H.W., Abele, D., Stefels, J., Van Leeuwe, M.A., Brussaard, C.P.D., Buma, A.G.J., Kohut, J., Sahade, R., Friedlaender, A.S., Stammerjohn, S.E., Venables, H.J., Meredith, M.P., 2019. Variability and change in the west Antarctic Peninsula marine system: Research priorities and opportunities. *Progress in Oceanography* 173, 208–237.
- Hernández, E.A., Piquet, A.M.T., Lopez, J.L., Buma, A.G.J., MacCormack, W.P., 2015. Marine archaeal community structure from Potter Cove, Antarctica: high temporal and spatial dominance of the phylum Thaumarchaeota. *Polar Biology* 38, 117–130.
- Hertzberg, J.E., Schmidt, M.W., Bianchi, T.S., Smith, R.K., Shields, M.R., Marcantonio, F., 2016. Comparison of eastern tropical Pacific TEX86 and Globigerinoides ruber Mg/Ca derived sea surface temperatures: Insights from the Holocene and Last Glacial Maximum. *Earth and Planetary Science Letters* 434, 320–332.
- Ho, S.L., Mollenhauer, G., Fietz, S., Martínez-García, A., Lamy, F., Rueda, G.,

- Schipper, K., Méheust, M., Rosell-Melé, A., Stein, R., Tiedemann, R., 2014. Appraisal of TEX86 and TEX86L thermometries in subpolar and polar regions. *Geochimica et Cosmochimica Acta* 131, 213–226.
- Hopmans, E.C., Weijers, J.W.H., Schefuß, E., Herfort, L., Sinninghe Damsté, J.S., Schouten, S., 2004. A novel proxy for terrestrial organic matter in sediments based on branched and isoprenoid tetraether lipids. *Earth and Planetary Science Letters* 224, 107–116.
- Huai, B., Wang, Y., Ding, M., Zhang, J., Dong, X., 2019. An assessment of recent global atmospheric reanalyses for Antarctic near surface air temperature. *Atmospheric Research* 226, 181–191.
- Huang, J., Sun, L., Wang, X., Wang, Y., Huang, T., 2011. Ecosystem evolution of seal colony and the influencing factors in the 20th century on Fildes Peninsula, West Antarctica. *Journal of Environmental Sciences* 23, 1431–1436.
- Hurley, S.J., Lipp, J.S., Close, H.G., Hinrichs, K.U., Pearson, A., 2018. Distribution and export of isoprenoid tetraether lipids in suspended particulate matter from the water column of the Western Atlantic Ocean. *Organic Geochemistry* 116, 90–102.
- Jaeschke, A., Wengler, M., Hefter, J., Ronge, T.A., Geibert, W., Mollenhauer, G., Gersonde, R., Lamy, F., 2017. A biomarker perspective on dust, productivity, and sea surface temperature in the Pacific sector of the Southern Ocean. *Geochimica et Cosmochimica Acta* 204, 120–139.
- Kaur, G., Mountain, B.W., Stott, M.B., Hopmans, E.C., Pancost, R.D., 2015. Temperature and pH control on lipid composition of silica sinters from diverse hot springs in the Taupo Volcanic Zone, New Zealand. *Extremophiles* 19, 327–344.
- Kejna, M., Arażny, A., Sobota, I., 2013. Climatic change on King George Island in the years 1948 – 2011. *Polish Polar Research* 34, 213–235.
- Kim, J.H., van der Meer, J., Schouten, S., Helmke, P., Willmott, V., Sangiorgi, F., Koç, N., Hopmans, E.C., Sinninghe Damsté, J.S., 2010. New indices and calibrations derived from the distribution of crenarchaeal isoprenoid tetraether lipids: Implications for past sea surface temperature reconstructions. *Geochimica et Cosmochimica Acta* 74, 4639–4654.
- Lange, P.K., Tenenbaum, D.R., Tavano, V.M., Paranhos, R., Campos, L.S., 2015. Shifts in microphytoplankton species and cell size at Admiralty Bay, Antarctica. *Antarctic Science* 27, 225–239.
- Machado, A., Chemale Jr., F., Lima, E.F., Figueiredo, A.M.G., 1998. Petrologia das

- rochas vulcânicas da Península Fildes, Ilha Rei George, Antártica. *Pesquisas em Geociências* 25, 35–42.
- Machado, A., Lima, E.F., Chemale Jr., F., Liz, J.D., Ávila, J.N., 2001. Química mineral das rochas vulcânicas da Península Fildes (Ilha Rei George), Antártica. *Revista Brasileira de Geociências* 31, 299–306.
- Martins, C.C., Aguiar, S.N., Wisnieski, E., Ceschim, L.M.M., Figueira, R.C.L., Montone, R.C., 2014. Baseline concentrations of faecal sterols and assessment of sewage input into different inlets of Admiralty Bay, King George Island, Antarctica. *Marine Pollution Bulletin* 78, 218–23.
- Martins, C.C., Bicego, M.C., Rose, N.L., Taniguchi, S., Lourenço, R.A., Figueira, R.C.L., Mahiques, M.M., Montone, R.C., 2010. Historical record of polycyclic aromatic hydrocarbons (PAHs) and spheroidal carbonaceous particles (SCPs) in marine sediment cores from Admiralty Bay, King George Island, Antarctica. *Environmental Pollution* 158, 192–200.
- Martins, C.C., Montone, R.C., Gamba, R.C., Pellizari, V.H., 2005. Sterols and fecal indicator microorganisms in sediments from Admiralty Bay, Antarctica. *Brazilian Journal of Oceanography* 53, 1–12.
- Nakayama, C.R., Kuhn, E., Araújo, A.C. V., Alvalá, P.C., Ferreira, W.J., Vazoller, R.F., Pellizari, V.H., 2011. Revealing archaeal diversity patterns and methane fluxes in Admiralty Bay, King George Island, and their association to Brazilian Antarctic Station activities. *Deep-Sea Research Part II: Topical Studies in Oceanography* 58, 128–138.
- Nędzarek, A., 2008. Sources, diversity and circulation of biogenic compounds in Admiralty Bay, King George Island, Antarctica. *Antarctic Science* 20, 135–145.
- Oliveira, M.A.G. de, Rosa, K.K., Vieira, R., Simões, J.C., 2019. Variação de área das geleiras do campo de gelo Kraków, Ilha Rei George, Antártica, no período entre 1956-2017. *Revista Caminhos de Geografia* 20, 55–71.
- Park, E., Hefter, J., Fischer, G., Hvitfeldt Iversen, M., Ramondenc, S., Nöthig, E.M., Mollenhauer, G., 2019. Seasonality of archaeal lipid flux and GDGT-based thermometry in sinking particles of high-latitude oceans: Fram Strait (79°N) and Antarctic Polar Front (50°S). *Biogeosciences* 16, 2247–2268.
- Park, E., Hefter, J., Fischer, G., Mollenhauer, G., 2018. TEX86 in sinking particles in three eastern Atlantic upwelling regimes. *Organic Geochemistry* 124, 151–163.
- Pearson, A., Huang, Z., Ingalls, A.E., Romanek, C.S., Wiegel, J., Freeman, K.H.,

- Smittenberg, R.H., Zhang, C.L., 2004. Nonmarine crenarchaeol in Nevada hot springs. *Applied and Environmental Microbiology* 70, 5229–5237.
- Petrick, B.F., McClymont, E.L., Littler, K., Rosell-Melé, A., Clarkson, M.O., Maslin, M., Röhl, U., Shevenell, A.E., Pancost, R.D., 2018. Oceanographic and climatic evolution of the southeastern subtropical Atlantic over the last 3.5 Ma. *Earth and Planetary Science Letters* 492, 12–21.
- Pichlmaier, M., Aquino, F.E., Silva, C.S. da, Braun, M.H., 2004. Suspended sediments in Admiralty Bay, King George Island (Antarctica). *Pesquisa Antártica Brasileira* 85, 77–85.
- QGIS Development Team, 2018. QGIS Geographic Information System. Open Source Geospatial Foundation Project.
- R Core Team, 2018. R: A language and environment for statistical computing.
- Rakusa-Suszczewski, S., 1995. The hydrography of Admiralty Bay and its inlets, coves and lagoons (King George Island, Antarctica). *Polish Polar Research* 16, 61–70.
- Robakiewicz, M., Rakusa-Suszczewski, S., 1999. Application of 3D circulation model to Admiralty Bay, King George Island, Antarctica. *Polish Polar Research* 20, 43–58.
- Robinson, S.A., Ruhl, M., Astley, D.L., Naafs, B.D.A., Farnsworth, A.J., Bown, P.R., Jenkyns, H.C., Lunt, D.J., O’Brien, C., Pancost, R.D., Markwick, P.J., 2017. Early Jurassic North Atlantic sea-surface temperatures from TEX86 palaeothermometry. *Sedimentology* 64, 215–230.
- Roesch, A., Schmidbauer, H., 2018. WaveletComp: Computational Wavelet Analysis, v. 1.1.
- Rosa, K.K., Freiburger, V.L., Vieira, R., Rosa, C.A., Simões, J.C., 2014. Glacial recent changes and climate variability in King George Island, Antarctica. *Quaternary and Environmental Geosciences* 05, 176–183.
- Rückamp, M., Braun, M.H., Suckro, S., Blindow, N., 2011. Observed glacial changes on the King George Island ice cap, Antarctica, in the last decade. *Global and Planetary Change* 79, 99–109.
- SCAR Reader Project, 2019. Surface meteorology at British Antarctic Survey Stations, 1947-2013 [WWW Document]. URL <https://legacy.bas.ac.uk/met/READER/> (accessed 10.24.19).
- Schouten, S., Hopmans, E.C., Schefuß, E., Sinninghe Damsté, J.S., 2002. Distributional variations in marine crenarchaeol membrane lipids: a new tool for reconstructing

ancient sea water temperatures? *Earth and Planetary Science Letters* 204, 265–274.

Schouten, S., Hopmans, E.C., Sinninghe Damsté, J.S., 2013. The organic geochemistry of glycerol dialkyl glycerol tetraether lipids: A review. *Organic Geochemistry* 54, 19–61.

Shetye, S., Jena, B., Mohan, R., 2017. Dynamics of sea-ice biogeochemistry in the coastal Antarctica during transition from summer to winter. *Geoscience Frontiers* 8, 507–516.

Shevenell, A.E., Ingalls, A.E., Domack, E.W., Kelly, C., 2011. Holocene Southern Ocean surface temperature variability west of the Antarctic Peninsula. *Nature* 470, 250–254.

Signori, C.N., Pellizari, V.H., Enrich-Prast, A., Sievert, S.M., 2018. Spatiotemporal dynamics of marine bacterial and archaeal communities in surface waters off the northern Antarctic Peninsula. *Deep-Sea Research Part II: Topical Studies in Oceanography* 149, 150–160.

Simões, J.C., Bremer, U.F., Aquino, F.E., Ferron, F.A., 1999. Morphology and variations of glacial drainage basins in the King George Island ice field, Antarctica. *Annals of Glaciology* 29, 220–224.

Sinninghe Damsté, J.S., Ossebaer, J., Schouten, S., Verschuren, D., 2012. Distribution of tetraether lipids in the 25-ka sedimentary record of Lake Challa: extracting reliable TEX86 and MBT/CBT palaeotemperatures from an equatorial African lake. *Quaternary Science Reviews* 50, 43–54.

Smellie, J.L., Pankhurst, R.J., Thomson, M.R.A., Davies, R.E.S., 1984. The geology of the South Shetland Islands: VI. Stratigraphy, geochemistry and evolution., in: *British Antarctic Survey Scientific Reports*. Cambridge, p. 85.

Tierney, J.E., Tingley, M.P., 2014. A Bayesian, spatially-varying calibration model for the TEX86 proxy. *Geochimica et Cosmochimica Acta* 127, 83–106.

Turner, J., Lu, H., White, I., King, J.C., Phillips, T., Hosking, J.S., Bracegirdle, T.J., Marshall, G.J., Mulvaney, R., Deb, P., 2016. Absence of 21st century warming on Antarctic Peninsula consistent with natural variability. *Nature* 535, 411–415.

Volkman, J.K., 1986. A review of sterol markers for marine and terrigenous organic matter. *Organic Geochemistry* 9, 83–99.

Volkman, J.K., 2006. Lipid markers for marine organic matter, in: Volkman, J.K. (Ed.), *Marine Organic Matter: Biomarkers, Isotopes and DNA. The Handbook of Environmental Chemistry, Vol 2N*. Springer, Berlin, Heidelberg, pp. 27–70.

- Volkman, J.K., Revill, A.T., Holdsworth, D.G., Fredericks, D., 2008. Organic matter sources in an enclosed coastal inlet assessed using lipid biomarkers and stable isotopes. *Organic Geochemistry* 39, 689–710.
- Wakeham, S.G., Canuel, E.A., 2006. Degradation and preservation of organic matter in marine sediments, in: Volkman, J.K. (Ed.), *Marine Organic Matter: Biomarkers, Isotopes and DNA. The Handbook of Environmental Chemistry, Vol 2N*. Springer Berlin Heidelberg, Berlin, Heidelberg, pp. 295–321.
- Weber, R.R., Montone, R.C., 2006. Rede 2 - Gerenciamento ambiental na Baía do Almirantado, Ilha Rei George, Antártica.
- Weijers, J.W.H., Schouten, S., Spaargaren, O.C., Sinninghe Damsté, J.S., 2006. Occurrence and distribution of tetraether membrane lipids in soils: Implications for the use of the TEX86 proxy and the BIT index. *Organic Geochemistry* 37, 1680–1693.
- Wisniewski, E., Bicego, M.C., Montone, R.C., Figueira, R.C.L., Ceschim, L.M.M., Mahiques, M.M., Martins, C.C., 2014. Characterization of sources and temporal variation in the organic matter input indicated by n-alkanols and sterols in sediment cores from Admiralty Bay, King George Island, Antarctica. *Polar Biology* 37, 483–496.
- Zhang, Y.G., Pagani, M., Wang, Z., 2016. Ring Index: A new strategy to evaluate the integrity of TEX86 paleothermometry. *Paleoceanography* 31, 220–232.
- Zhang, Y.G., Zhang, C.L., Liu, X.-L., Li, L., Hinrichs, K.U., Noakes, J.E., 2011. Methane Index: A tetraether archaeal lipid biomarker indicator for detecting the instability of marine gas hydrates. *Earth and Planetary Science Letters* 307, 525–534.

Figure Captions

Fig. 1. Map of the study area with the location of the sediment cores collected in Admiralty Bay, Antarctic Peninsula. The red dots represent the location of the sediment cores, the blue diamonds represent glaciers mentioned in the Discussion, and the red triangle represents the Russian Bellingshausen research station.

Fig. 2. Profiles and trends (based on linear models between 1963 and 1975, 1975 and 1998, and 1998 and 2006; dashed lines) of the total organic carbon (TOC, in %), total sterols (in $\mu\text{g g}^{-1}$), total alcohols (in $\mu\text{g g}^{-1}$), and isoprenoid GDGTs (in $\mu\text{g g}^{-1}$) in the BTP sediment core.

Fig. 3. Profiles of the main sterols, the fatty aliphatic alcohols and the main isoprenoid GDGTs (all data in $\mu\text{g g}^{-1}$); and the ratio of 5α -stanols/ Δ^5 -stenols in the BTP sediment core. The vertical dashed gray line indicates the threshold of diagenesis (Wakeham and Canuel, 2006).

Fig. 4. Comparison between GDGT-based sea surface temperatures (SST) from our short marine sediment cores and instrumental temperatures from SODA3 reanalysis. The red line represents the mean austral spring (OND) temperature, while the red band represents the annual variation. Regarding the GDGT-based SST estimates, the line represents the calculated SST using five different calibrations (from left to right: $\text{TEX}_{86}^{\text{L}}$, AntPen, Bayspar, $\text{TEX}_{86}^{\text{L}}$ quad and OPTiMAL), while the bands represent the calibration errors (from left to right: $\text{TEX}_{86}^{\text{L}} = \pm 4\text{ }^{\circ}\text{C}$, AntPen = $\pm 2.2\text{ }^{\circ}\text{C}$, Bayspar = $\pm 5\text{ }^{\circ}\text{C}$, $\text{TEX}_{86}^{\text{L}}$ quad = $\pm 5\text{ }^{\circ}\text{C}$ and OPTiMAL = $\pm 3.4\text{ }^{\circ}\text{C}$).

Fig. 5. Profiles of the normalized proxies of organic matter (total sterols, total alcohols and isoGDGTs), sea surface temperature (in $^{\circ}\text{C}$), seasonal means of wind speed in Bellingshausen (in m s^{-1}), seasonal mean of precipitation in Bellingshausen (in mm), and area loss of the main glaciers around Botany Point (in km^2). The trends (colored dashed lines) are based on linear models between 1963 and 1975, 1975 and 1998, and 1998 and 2006.

Fig. 6. Comparison between GDGT-based sea surface temperatures from Botany Point (BTP) and mean annual air temperatures from King George Island based on Kejna et al. (2013). (Top panel) The band represents the calibration error ($\pm 5^{\circ}\text{C}$), while the error bars in the x-axis represent the age model uncertainties. (Bottom panel) Trends (based on linear models) between the periods: 1963 – 1975, 1975 – 1998 and 1998 – 2006 (2011 in the MAT data).

Table Captions

Table 1. Sediment cores collected at Admiralty Bay, King George Island, Antarctica. LSR = Mean post-1963 estimated linear sedimentation rates.

Table 2. Spearman correlation analysis between GDGTs-based sea surface temperatures (considering the three records combined) and mean annual and austral seasonal temperatures from SODA3 reanalysis. $x = p\text{-value} < 0.05$. JFM = austral summer, AMJ = austral autumn, JAS = austral winter, OND = austral spring. Calibrations: TEX₈₆^L based on Kim et al. (2010); AntPen based on Shevenell et al. (2011); Bayspar based on Tierney and Tingley (2014); TEX₈₆^L quad based on Park et al. (2019) and OPTiMAL based on Dunkley Jones et al. (2020).

Exploring the application of TEX₈₆ and the sources of organic matter in the Antarctic coastal region

Ana Lúcia L. Dauner, B. David A. Naafs, Richard D. Pancost, César C. Martins

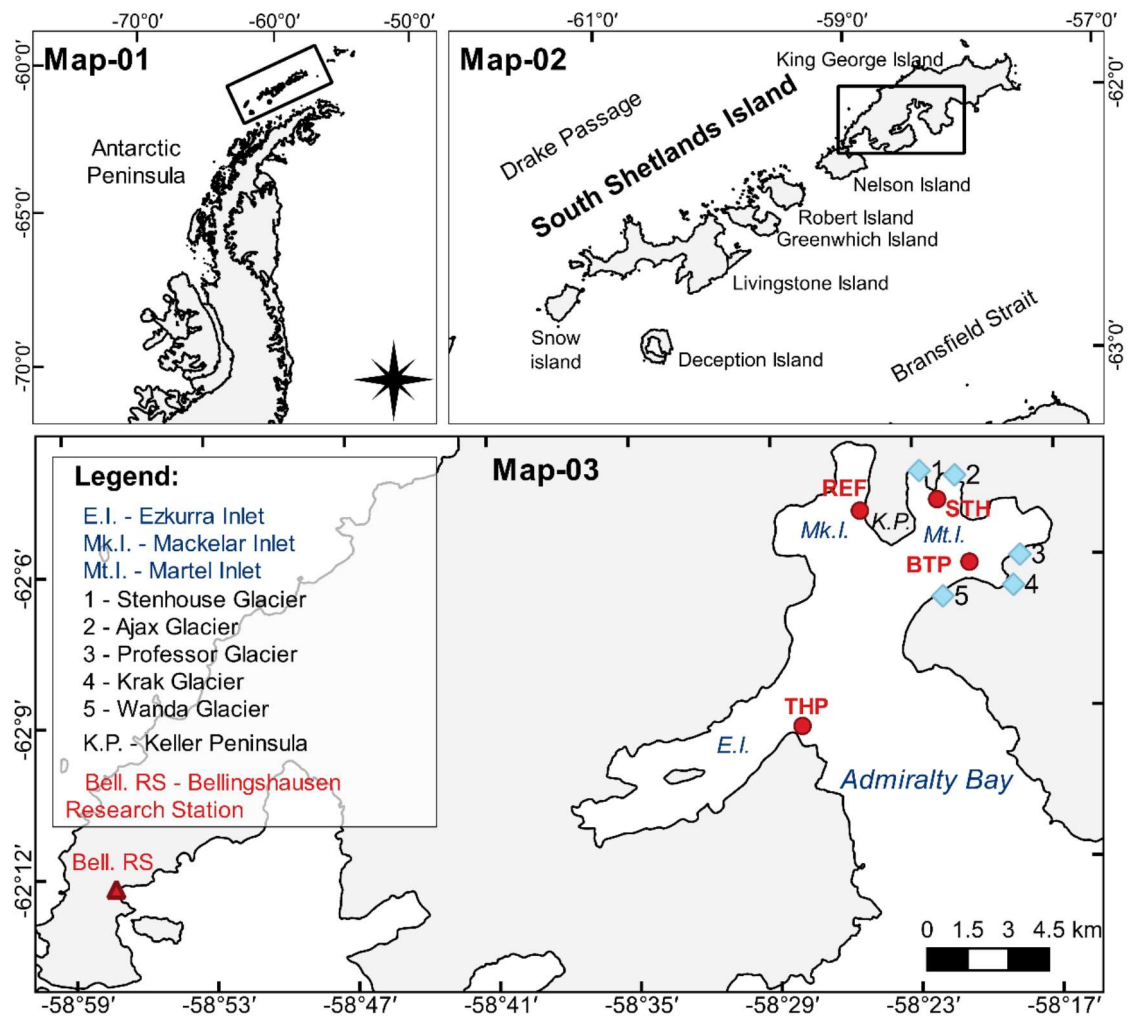


Fig. 1

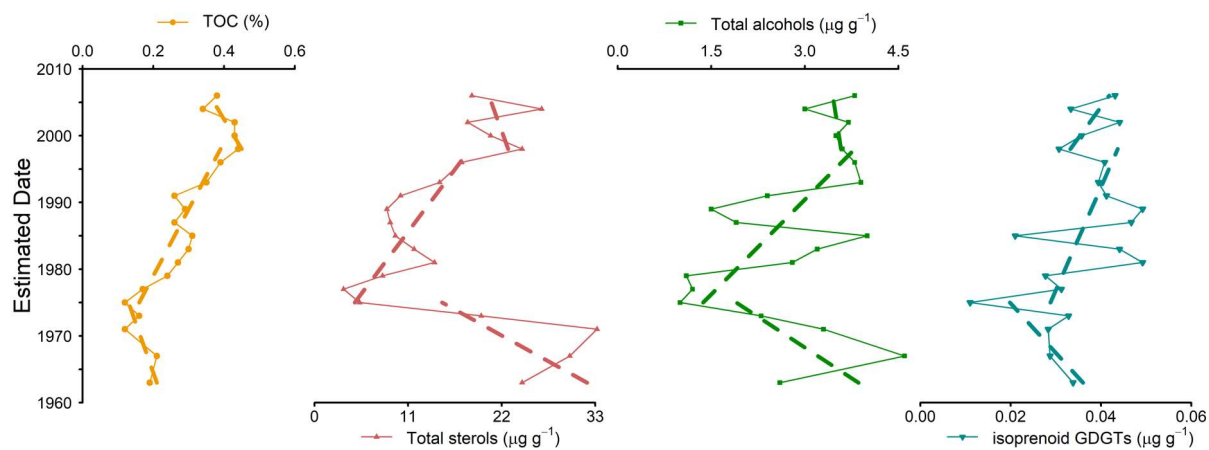


Fig. 2

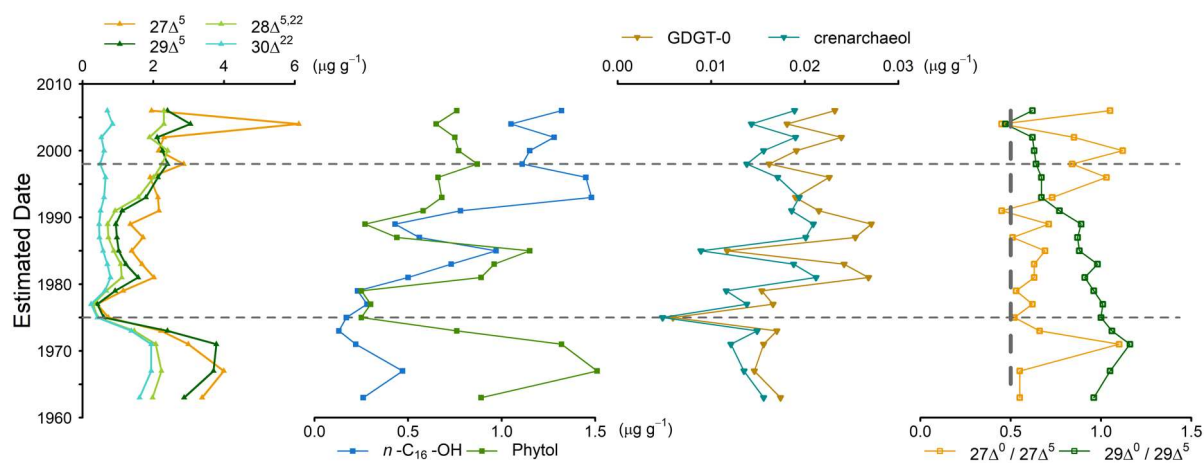


Fig. 3

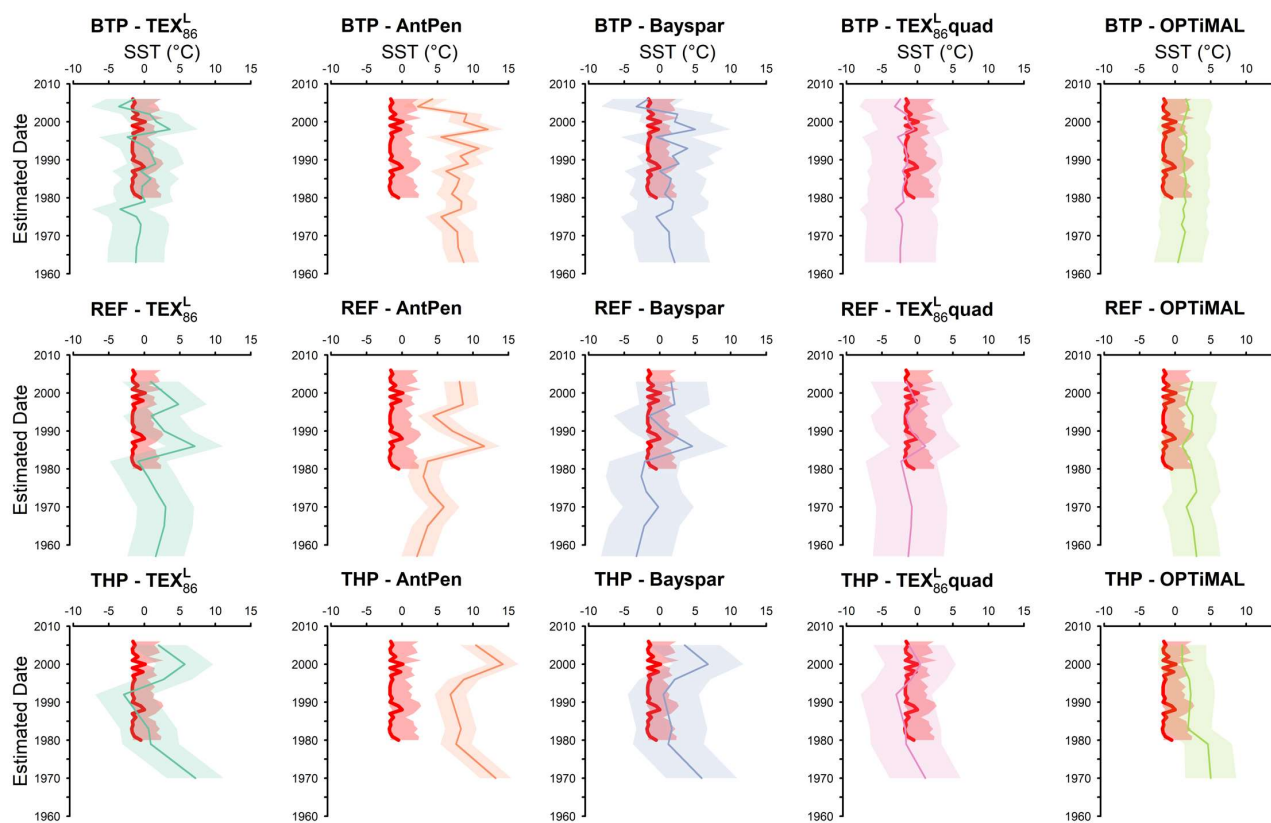


Fig. 4

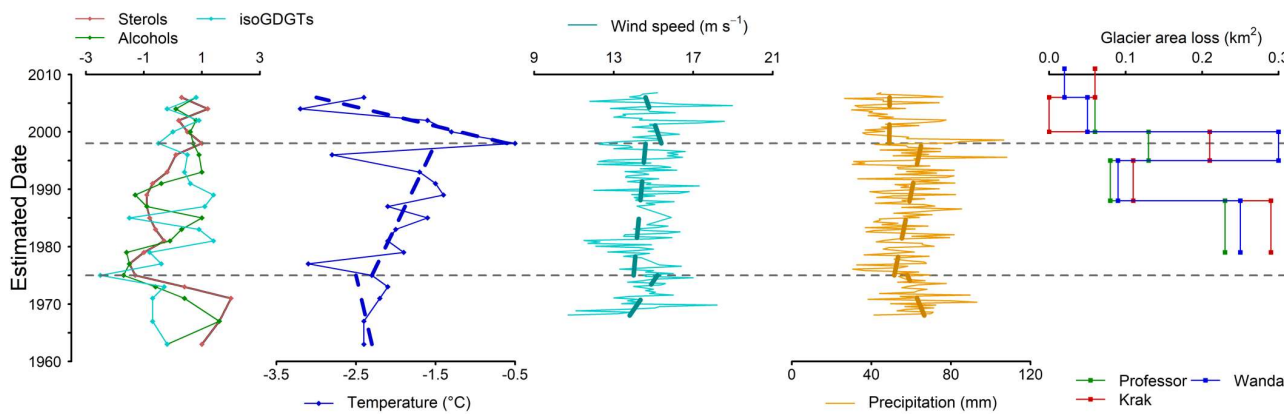


Fig. 5

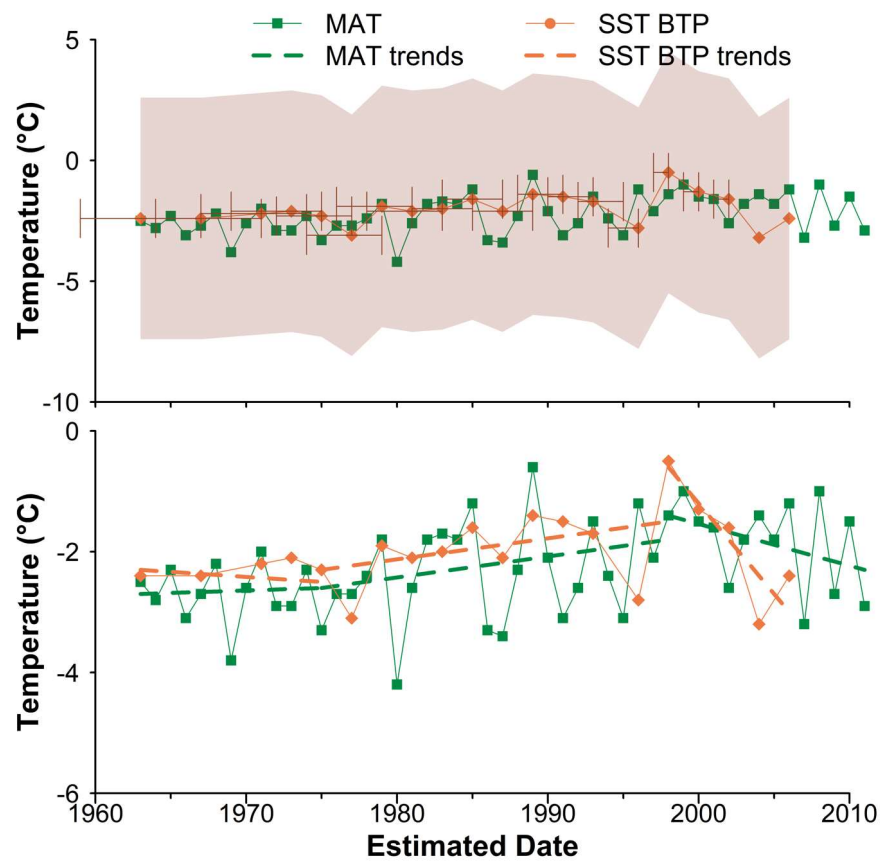


Fig. 6

Exploring the application of TEX₈₆ and the sources of organic matter in the Antarctic coastal region

Ana Lúcia L. Dauner, B. David A. Naafs, Richard D. Pancost, César C. Martins

Table 1. Sediment cores collected at Admiralty Bay, King George Island, Antarctica.
LSR = Mean post-1963 estimated linear sedimentation rates.

Site	Name	Latitude	Longitude	Depth (m)	LSR (cm yr ⁻¹)
BTP	Botany Point	- 62.09718	- 58.35078	30	0.48 ^a
REF	Refuge II	- 62.07952	- 58.42745	20	0.26 ^b
STH	Stenhouse Glacier	- 62.07625	- 58.37270	25	0.42 ^a
THP	Thomas Point	- 62.15040	- 58.47140	20	0.23 ^b

^a Ferreira et al. (2013); ^b Martins et al. (2014)

Table 2. Spearman correlation analysis between GDGTs-based sea surface temperatures (considering the three records combined) and mean annual and austral seasonal temperatures from SODA3 reanalysis. x = p -value < 0.05. JFM = austral summer, AMJ = austral autumn, JAS = austral winter, OND = austral spring. Calibrations: TEX₈₆^L based on Kim et al. (2010); AntPen based on Shevenell et al. (2011); Bayspar based on Tierney and Tingley (2014); TEX₈₆^L quad based on Park et al. (2019) and OPTiMAL based on Dunkley Jones et al. (2020).

Calibration	Annual	JFM	AMJ	JAS	OND
TEX ₈₆ ^L	x	x	x	x	0.54
AntPen	x	- 0.44	x	x	0.61
Bayspar	x	- 0.44	x	x	0.61
TEX ₈₆ ^L quad	x	x	x	x	0.56
OPTiMAL	x	x	x	x	- 0.60